

# A variable threshold visual sensing and image reconstruction method based on pulse sequence

Jiangtao XU<sup>1,2</sup>, Peng LIN<sup>1,2</sup>, Zhiyuan GAO<sup>1,2\*</sup>, Kaiming NIE<sup>1,2</sup> & Liang XU<sup>1,2</sup>

<sup>1</sup>School of Microelectronics, Tianjin University, Tianjin 300072, China;

<sup>2</sup>Tianjin Key Laboratory of Imaging and Sensing Microelectronic Technology, Tianjin 300072, China

Received 24 April 2020/Revised 17 July 2020/Accepted 23 July 2020/Published online 22 February 2021

**Citation** Xu J T, Lin P, Gao Z Y, et al. A variable threshold visual sensing and image reconstruction method based on pulse sequence. *Sci China Inf Sci*, 2022, 65(2): 129401, <https://doi.org/10.1007/s11432-020-3003-2>

Dear editor,

Pulsed-based CMOS image sensor (CIS) outperforms classic CIS in terms of data rate, and is able to achieve ultra-high-speed imaging [1]. A pulsed-based CIS which is able to capture the movement of the hard disk rotating at 6000 r/min, was designed in our previous work [2,3]. The main problems of the pulse-based sensing mechanism are nonlinearity and readout noise.

**Nonlinearity.** As light intensity is inversely proportional to the pulse interval [4], reconstructed images will involve loss of gray levels or lag in various light conditions [5].

**Readout noise.** In the synchronous readout operation, there is a waiting time between pixel trigger and pulse readout, which can be treated as readout noise [1, 6].

Detailed operation principle and error analysis of the pulsed-based sensing scheme are given in Appendix A.

In this study, we propose a variable threshold visual sensing and image reconstruction method based on pulse sequence. Threshold varying with time alters the range of light intensity mapped to a specific range of digital codes [7]. By analyzing pulse information in different trigger cycles, the proposed method is able to suppress the readout noise and reconstruct richer gray information.

The structure and working process of the spiking pixel based on variable threshold are shown in Figure 1. The threshold curve consists of periodic ramps. Each ramp consists of many small steps, whose width is set equal to frame period  $T_u$  and height is written as  $V_s$ . The threshold voltage linearly increases from minimum value  $V_{th0}$  to maximum value  $V_{th,max}$  by step height  $V_s$  every frame cycle during a ramp cycle. Every time a new ramp cycle starts, a ramp pulse is output by a global ramp generator.

The pixel consists of a reset transistor, a photodiode (PD), a comparator, a latch and an output stage. When the voltage on PD reaches  $V_{th,i}$ , the comparator outputs a pulse. Then the PD is reset to  $V_{rst}$  when the row selection signal arrives. The row selection signal picks the pixel and the trigger state is read out through the column bus every other frame cycle. The process from the start of integra-

tion to the readout of the triggered pulse is defined as a trigger cycle. After  $N_i$  frame cycles, the voltage on PD is integrated to the threshold  $V_{th,i+1}$  and the pixel is triggered again.  $N_i$  and  $V_{th,i}$  are called the trigger interval and the trigger threshold of  $i$ -th trigger cycle, respectively.

**Proposition 1.** In the  $i$ -th trigger cycle, input photocurrent  $I_{ph}$  satisfies

$$\frac{C_{PD}(V_{rst} - V_{th,i})}{N_i \cdot T_u} < I_{ph} \leq \frac{C_{PD}(V_{rst} - V_{th,i} + V_s)}{(N_i - 1) \cdot T_u}, \quad (1)$$

where  $C_{PD}$  is the parasitic capacitance of PD.

**Definition 1.** Consecutive trigger cycles where the illumination keeps constant are defined as a trigger window. Parameter  $n$  represents the number of trigger cycles in the trigger window and is called window depth.

In a trigger window, the restored photocurrent,  $I_{cal}$ , is in the intersection set of different ranges calculated by (1) in different trigger cycles. The lower limit and the higher limit of restored photocurrent in the trigger window are written as  $I_{min}$  and  $I_{max}$ , respectively.

**Definition 2.** Equivalent trigger interval is defined as the trigger interval of the pixel integrated from  $V_{rst}$  to  $V_{th0}$ .  $N_{equ,m}$ ,  $N_{equ,g}$ , and  $N_{equ}$  are the equivalent trigger interval at  $I_{min}$ ,  $I_{max}$ , and  $I_{cal}$ , respectively.

We take the average of  $I_{min}$  and  $I_{max}$  as the restored photocurrent. According to Definition 2, the restored photocurrent is given by

$$I_{cal} = C_{PD} (V_{rst} - V_{th0}) / (N_{equ} \cdot T_u). \quad (2)$$

The final gray value of the image is given by

$$Y = \left[ \left( 2^{N_{id}} - 1 \right) I_{cal} / I_{pmax} \right] = \left[ \left( 2^{N_{id}} - 1 \right) N_{max} / N_{equ} \right], \quad (3)$$

where  $N_{id}$  is image depth,  $I_{pmax}$  is the input photocurrent mapped to the largest gray value,  $N_{max}$  is the equivalent trigger interval at  $I_{pmax}$ .

\* Corresponding author (email: gaozhiyuan@tju.edu.cn)

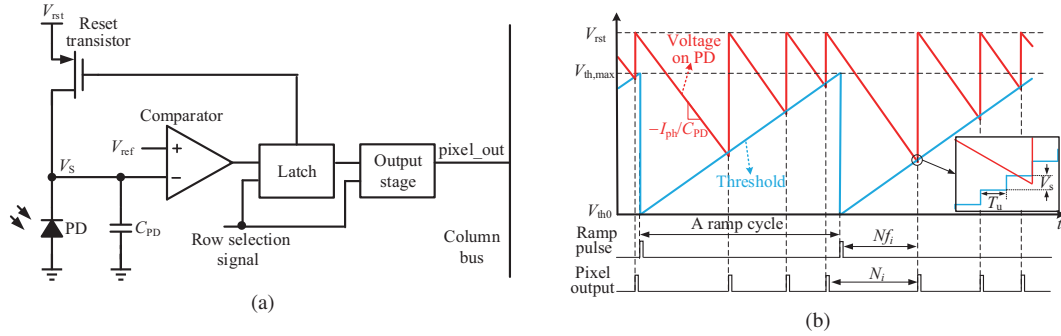


**Figure 1** (Color online) (a) The structure of the pixel; (b) the working process of pixel with variable threshold.

**Proposition 2.** In a trigger window,  $N_{\text{equ}}$  is given by

$$N_{\text{equ}} = 2N_{\text{equ},g}N_{\text{equ},m}/(N_{\text{equ},g} + N_{\text{equ},m}). \quad (4)$$

And  $N_{\text{equ},m}$  and  $N_{\text{equ},g}$  are calculated by

$$N_{\text{equ},m} = \min \{N_i/(1 - a \cdot Nf_i)\}, \quad (5)$$

$$N_{\text{equ},g} = \max \{(N_i - 1)/(1 - a(Nf_i - 1))\}, \quad (6)$$

where  $i$  is an integer varying from 1 to  $n$ ,  $Nf_i$  is the interval between the pixel pulse output in the  $i$ -th trigger cycle and the immediately prior ramp pulse,  $a$  is system parameter given by

$$a = V_s/(V_{\text{rst}} - V_{\text{th0}}). \quad (7)$$

By information of pixel pulses and ramp pulses, we can easily obtain the equivalent trigger intervals of arbitrary trigger window. Then the restored photocurrent and the gray level can be obtained according to (2) and (3), respectively.

**Remark 1.** In the reconstruction of static scene, window depth can be large enough to minimize readout noise and information loss. As window depth increases, the calculated  $N_{\text{equ},m}$  and  $N_{\text{equ},g}$  will get closer. Then the  $N_{\text{equ}}$  can be restored more accurately and the restored photocurrent will be closer to the actual input photocurrent, leading to lower readout noise and richer reconstructed information.

In the reconstruction of dynamic scenes, window depth is limited by the dynamic photocurrent. An optimal window depth is the key to ensure the effective acquisition of dynamic object information.

**Proposition 3.** In the reconstruction of dynamic scenes, the illumination is considered constant in the case of

$$\frac{N_{i+1} - \zeta}{N_i} < \frac{1 - a \cdot Nf_{i+1}}{1 - a \cdot Nf_i} < \frac{N_{i+1}}{N_i - \zeta}, \quad (8)$$

where  $\zeta$  is the error tolerance and is set in the range of 0 to 1.

The proof of Propositions 1–3 is given in Appendix B.

If  $N_{i-1}$  and  $N_i$  satisfy (8), the  $(i-1)$ -th and  $i$ -th trigger cycles are involved in the same trigger window. If  $N_{i-1}$  and  $N_i$  satisfy (8) whereas  $N_i$  and  $N_{i+1}$  do not, it can be inferred that the photocurrent changes during the  $(i+1)$ -th trigger cycle and the  $(i+1)$ -th trigger cycle is involved in another trigger window.

**Remark 2.** In the reconstruction of dynamic scenes, the method automatically judges whether the received photocurrent changes, and adaptively determines the window

depth. The smaller  $\zeta$  is, the more sensitive the method is to photocurrent change, and the greater the effect of readout noise on window depth is.

**Experiment.** To verify the effectiveness of the proposed reconstruction method, behavioral models of visual sensing based on fixed threshold and variable threshold are built, respectively. The experiment results are given in Appendix C.

**Conclusion.** This study presents a variable threshold visual sensing scheme based on pulse sequence. Corresponding image reconstruction method for both static scene and dynamic scene is also proposed. The threshold keeps constant within one frame period and varies with predefined step height in different frame cycles. Combining pulse sequence with variable threshold enables pulse information to change with trigger cycles even in constant illumination. By analyzing the pulse information in different trigger cycles, readout noise is suppressed, and richer information is reconstructed.

**Acknowledgements** This work was supported by National Key R&D Program of China (Grant No. 2019YFB2204300).

**Supporting information** Appendixes A–C. The supporting information is available online at [info.scichina.com](http://info.scichina.com) and [link.springer.com](http://link.springer.com). The supporting materials are published as submitted, without typesetting or editing. The responsibility for scientific accuracy and content remains entirely with the authors.

## References

- Chen D G, Matolin D, Bermak A, et al. Pulse-modulation imaging-review and performance analysis. *IEEE Trans Biomed Circ Syst*, 2011, 5: 64–82
- Gao J, Wang Y Z, Nie K M, et al. The analysis and suppressing of non-uniformity in a high-speed spike-based image sensor. *Sensors*, 2018, 18: 4232
- Xu J T, Zhang P W, Yang Z, et al. Image lag elimination algorithm for pulse-sequence-based high-speed image sensor. *IEEE Access*, 2019, 7: 159575–159583
- Leñero-Bardallo J A, García-Pacheco F J. Fast luminance measurement method for asynchronous spiking pixels. *Electron Lett*, 2018, 54: 492–494
- Xu J T, Yang Z, Gao Z, et al. A method of biomimetic visual perception and image reconstruction based on pulse sequence of events. *IEEE Sens J*, 2019, 19: 1008–1018
- Tsai T H, Hornsey R. Analysis of dynamic range, linearity, and noise of a pulse-frequency modulation pixel. *IEEE Trans Electron Dev*, 2012, 59: 2675–2681
- Astrom A, Forchheimer R, Danielsson P E. Intensity mappings within the context of near-sensor image processing. *IEEE Trans Image Process*, 1998, 7: 1736–1741